



HAL
open science

Does chlorophyll a provide the best index of phytoplankton biomass for primary productivity studies?

Y. Huot, M. Babin, F. Bruyant, C. Grob, M. S. Twardowski, Hervé Claustre

► **To cite this version:**

Y. Huot, M. Babin, F. Bruyant, C. Grob, M. S. Twardowski, et al.. Does chlorophyll a provide the best index of phytoplankton biomass for primary productivity studies?. *Biogeosciences Discussions*, 2007, 4 (2), pp.707-745. hal-00330232

HAL Id: hal-00330232

<https://hal.science/hal-00330232>

Submitted on 18 Jun 2008

HAL is a multi-disciplinary open access archive for the deposit and dissemination of scientific research documents, whether they are published or not. The documents may come from teaching and research institutions in France or abroad, or from public or private research centers.

L'archive ouverte pluridisciplinaire **HAL**, est destinée au dépôt et à la diffusion de documents scientifiques de niveau recherche, publiés ou non, émanant des établissements d'enseignement et de recherche français ou étrangers, des laboratoires publics ou privés.

Biogeosciences Discussions is the access reviewed discussion forum of *Biogeosciences*

Does chlorophyll *a* provide the best index of phytoplankton biomass for primary productivity studies?

Y. Huot^{1,2}, **M. Babin**^{1,2}, **F. Bruyant**³, **C. Grob**^{1,2}, **M. S. Twardowski**⁴, and **H. Claustre**^{1,2}

¹CNRS, Laboratoire d'Océanographie de Villefranche, 06230 Villefranche-sur-Mer, France

²Université Pierre et Marie Curie-Paris6, Laboratoire d'Océanographie de Villefranche, 06230 Villefranche-sur-Mer, France

³Dalhousie University, Department of Oceanography, 1355 Oxford Street, Halifax N.S. B3H 4J1, Canada

⁴WET Labs, Inc. Department of Research 165 Dean Knauss Dr., Narragansett, RI 02882, USA

Received: 20 February 2007 – Accepted: 24 February 2007 – Published: 1 March 2007

Correspondence to: Y. Huot (huot@obs-vlfr.fr)

Proxies of biomass for primary production

Y. Huot et al.

Title Page

Abstract

Introduction

Conclusions

References

Tables

Figures

◀

▶

◀

▶

Back

Close

Full Screen / Esc

Printer-friendly Version

Interactive Discussion

Abstract

Probably because it is a readily available ocean color product, almost all models of primary productivity use chlorophyll as their index of phytoplankton biomass. As other variables become more readily available, both from remote sensing and in situ autonomous platforms, we should ask if other indices of biomass might be preferable. Herein, we compare the accuracy of different proxies of phytoplankton biomass for estimating the maximum photosynthetic rate (P_{\max}) and the initial slope of the production versus irradiance (P vs. E) curve (α). The proxies compared are: the total chlorophyll a concentration (Tchl_a, the sum of chlorophyll a and divinyl chlorophyll), the phytoplankton absorption coefficient, the phytoplankton photosynthetic absorption coefficient, the active fluorescence in situ, the particulate scattering coefficient at 650 nm ($b_p(650)$), and the particulate backscattering coefficient at 650 nm ($b_{bp}(650)$). All of the data (about 170 P vs. E curves) were collected in the South Pacific Ocean. We find that when only the phytoplanktonic biomass proxies are available, $b_p(650)$ and Tchl_a are respectively the best estimators of P_{\max} and α . When additional variables are available, such as the depth of sampling, the irradiance at depth, or the temperature, Tchl_a becomes the best estimator of both P_{\max} and α . From a remote sensing perspective, error propagation analysis shows that, given the current algorithms errors for estimating $b_{bp}(650)$, Tchl_a remains the best estimator of P_{\max} .

1 Introduction

One of the main reasons for measuring the marine phytoplanktonic biomass is to estimate the rate of primary production (PP). Because it is colored, specific to, and shared amongst all primary producers, the most widely used proxy of phytoplankton biomass is the total chlorophyll *a* concentration (Tchl_a, the sum of chlorophyll a and divinyl chlorophyll a). The Tchl_a can be estimated remotely using ocean color satellites (e.g. O'Reilly et al., 1998), in situ with fluorometers (Lorenzen, 1966) or radiometers,

BGD

4, 707–745, 2007

Proxies of biomass for primary production

Y. Huot et al.

Title Page

Abstract

Introduction

Conclusions

References

Tables

Figures

◀

▶

◀

▶

Back

Close

Full Screen / Esc

Printer-friendly Version

Interactive Discussion

EGU

Proxies of biomass for primary production

Y. Huot et al.

Title Page

Abstract

Introduction

Conclusions

References

Tables

Figures

◀

▶

◀

▶

Back

Close

Full Screen / Esc

Printer-friendly Version

Interactive Discussion

or measured on discrete samples through high performance liquid chromatography (HPLC) analysis (Mantoura and Llewellyn, 1983), fluorometric (Yentsch and Menzel, 1963) or spectrophotometric methods (Jeffrey and Humphrey, 1975). However, due to the pronounced variability of its cellular content and its ratio with respect to phytoplankton carbon, the concentration of Tchl_a is a biased estimator of phytoplankton biomass as organic carbon (Cullen, 1982). This variability could also reduce our ability to estimate PP. Considering that Tchl_a is used in almost all models of PP, the main question we wish to address in this paper is: Does Tchl_a provide the best index of phytoplankton biomass for primary productivity studies?

Calculating primary productivity with a time or depth resolved model requires an estimate of the photosynthetic rate of the community from low to high irradiances. One common approach is to build a relationship describing the rate of photosynthesis as a function of irradiance (the P vs. E curve). The rate of photosynthesis is then calculated according to the irradiance at a given time and depth and then integrated with respect to both (e.g. Morel, 1991). Often, this calculation is carried out on a per chlorophyll *a* basis and subsequently multiplied by the measured or estimated chlorophyll *a* concentration.

A P vs. E curve can be constructed by incubating seawater samples enriched in ¹⁴C under different irradiance levels for tens of minutes to a few hours (Lewis and Smith, 1983). From these incubations, the photosynthetic rates of the community can be described as a function of incident scalar irradiance ($\overset{o}{E}$, $\mu\text{mol photon m}^{-2} \text{s}^{-1}$) using a saturating function with two parameters: α ($\text{mgC m}^{-3} \text{h}^{-1} [\mu\text{mol photon m}^{-2} \text{s}^{-1}]^{-1}$) which describes the initial slope; and P_{max} ($\text{mgC m}^{-3} \text{h}^{-1}$) which describes the region where photosynthesis is saturated by light. One functional form commonly used is

$$P = P_{\text{max}} \left[1 - \exp \left(-\overset{o}{E} \alpha / P_{\text{max}} \right) \right] + P_o, \quad (1)$$

where P_o ($\text{mgC m}^{-3} \text{h}^{-1}$), an intercept term, is sometimes used to improve the fits (e.g. MacIntyre and Cullen 2005). The saturation irradiance for photosynthesis, $E_k = P_{\text{max}} / \alpha$ ($\mu\text{mol m}^{-2} \text{s}^{-1}$), is defined with this functional form as the irradiance level at

which the curve reaches 63.2% of its maximum. If photodamage occurs during the measurement, a third parameter, β ($\text{gC m}^{-3} \text{h}^{-1} [\mu\text{mol m}^{-2} \text{s}^{-1}]^{-1}$), can be used to describe the reduction of photosynthesis at the highest irradiance due to incubation irradiance (Platt et al., 1980):

$$P = P_s \left[1 - \exp\left(-\frac{E}{P_s} \alpha\right) \right] \left[\exp\left(-\beta \frac{E}{P_s}\right) \right] + P_o, \quad (2)$$

where P_s ($\text{mgC m}^{-3} \text{h}^{-1}$) is an hypothetical maximum photosynthetic rate without photoinhibition and an analytic function of β , α and P_{\max} . Leaving P_o aside for now, P_{\max} and α are the two parameters required to describe the curve using Eq. (1), or in their biomass normalized form $P_{\max}^B = P_{\max}/B$ and $\alpha^B = \alpha/B$ where B is a biomass proxy (units vary). Again, Tchl_a is generally used for B. Because P_{\max}^B and α^B are highly variable in the environment, methods for estimating them to model PP on large scales include describing relationships with one environmental variable (e.g. Behrenfeld and Falkowski, 1997) or oceanographic conditions (e.g. Behrenfeld et al., 2002), assigning values for large and dynamic oceanic provinces (e.g. Platt and Sathyendranath, 1999 and references therein) or as a function of species composition (Claustre et al., 2005). Within this context, it follows that the best measure of phytoplankton biomass will be the measure that generates the least variability in the biomass normalized photosynthetic parameters with growth conditions and species composition, or a biomass index that produces highly predictable variability in these photosynthetic parameters.

Theory and laboratory experiments can provide some guidance in this quest for the best biomass proxy by providing simple relationships for both P_{\max} and α . The P_{\max} value depends on the concentration (n_{slowest} , m^{-3}) and the average maximum turnover time ($\bar{\tau}_{\text{slowest}}$, s atoms^{-1}) of the slowest constituent pool in the photosynthetic chain,

$$P_{\max} = 7.174 \times 10^{-17} \frac{n_{\text{slowest}}}{\bar{\tau}_{\text{slowest}}}, \quad (3)$$

where $7.174 \times 10^{-17} \text{ mgC atoms}^{-1} \text{ s h}^{-1}$ is the conversion factor from seconds to hours and mg of carbon to atoms.

Proxies of biomass for primary production

Y. Huot et al.

Title Page

Abstract

Introduction

Conclusions

References

Tables

Figures

◀

▶

◀

▶

Back

Close

Full Screen / Esc

Printer-friendly Version

Interactive Discussion

The initial slope of the photosynthesis irradiance curve is given by the product of the spectrally weighted photosynthetic absorption (m^{-1}),

$$\bar{a}_{ps} = \int_{400}^{700} a_{ps}(\lambda) \overset{\circ}{E}(\lambda) d\lambda \bigg/ \int_{400}^{700} \overset{\circ}{E}(\lambda) d\lambda, \quad (4)$$

and the maximum quantum yield of carbon fixation for photons absorbed by photosynthetic pigments ($\varphi_{C_{max}}^{ps}$, mol C [mol photons absorbed] $^{-1}$), as follows:

$$\alpha = 43.2 \bar{a}_{ps} \varphi_{C_{max}}^{ps}. \quad (5)$$

In Eq. (5), the factor $43.2 \text{ mg C mol C}^{-1} \text{ mol photons } \mu\text{mol photons}^{-1} \text{ s h}^{-1}$ accounts for the conversion from seconds to hours, $\mu\text{mol photons}$ to mol photons , and mg C to mol C . Both P_{max} and α are thus described by a different amount or “biomass” term ($n_{slowest}$ and \bar{a}_{ps}), and a term which encompasses variability in the physiological or photosynthetic efficiency ($\bar{\tau}_{slowest}$ and $\varphi_{C_{max}}^{ps}$). It follows that, in theory, the best measures of photosynthetic biomass are $n_{slowest}$ for the light-saturated region of the curve, and \bar{a}_{ps} for the light-limited region of the curve. Hence, because $n_{slowest}$ is not a pigmented molecule responsible for part of \bar{a}_{ps} (e.g., Suenic et al., 1987), even if $\bar{\tau}_{slowest}$ or $\varphi_{C_{max}}^{ps}$ remained constant, there is not a single measure of phytoplankton biomass which will lead to a constant shape of the biomass normalized PvsE curve. This is a well-known feature of the PvsE curve. For example, from an extensive review of the literature, MacIntyre et al. (2002) showed that for a given species under different photoacclimation states, Tchla (apparently a good proxy for \bar{a}_{ps}) is a better measure for the light-limited region and phytoplankton carbon (C_{phy}), apparently a good proxy for $n_{slowest}$, is a better measure of photosynthetic biomass at light saturation.

Progress in predicting P_{max} is central to making improvements in the estimation of primary production, as variability in depth-integrated primary production is believed to be mostly driven by the light-saturated rate of photosynthesis (Behrenfeld and Falkowski, 1997). This parameter is also one of the least well-constrained in primary production

Title Page

Abstract

Introduction

Conclusions

References

Tables

Figures

◀

▶

◀

▶

Back

Close

Full Screen / Esc

Printer-friendly Version

Interactive Discussion

models. Therefore, if it could be estimated accurately, phytoplankton carbon might provide an ideal alternative for primary production models and possibly reduce errors in the estimation of photosynthetic parameters, at least at high irradiance. Unfortunately, a direct measure of phytoplankton carbon in situ or from remote sensing does not exist.

5 However, other potentially useful proxies of phytoplankton carbon have been proposed.

These potentially useful measures include indirect optical methods. In particular, recent proposals by Behrenfeld and colleagues (Behrenfeld and Boss, 2003; Behrenfeld et al., 2005; Behrenfeld and Boss, 2006) suggesting that scattering-based measures could provide an accurate estimate of phytoplankton carbon, have brought to the fore-
10 front questions regarding the interpretation of these optical proxies of phytoplankton biomass. Though it has long been known that the beam attenuation coefficient (c_p , m^{-1} , essentially equal to the scattering coefficient in the red wavebands where it is generally measured) is a good proxy of the total particulate organic carbon (POC) in case 1 waters (Morel, 1988; Gardner et al., 2006 and references therein), the suggestion of
15 Behrenfeld and Boss (2003) that it represents an accurate proxy of phytoplankton carbon merits further research. In a similar way, the particulate backscattering coefficient (b_{bp} , m^{-1}), which can be obtained from satellite remote sensing, has been used to estimate the concentration of POC (Stramski et al., 1999). More recently, Behrenfeld et al. (2005) proposed the utilization of the backscattering coefficient to estimate the
20 phytoplankton carbon over large space and time scales. Because of its implications, the idea has already garnered significant attention (e.g. Smith, 2005). However, based on Mie theory calculations, backscattering is expected to be mostly influenced by non-phytoplanktonic, submicron particles (Morel and Ahn, 1991; Stramski et al., 2004), albeit the sources of backscattered light in the ocean remains controversial. Thus, it
25 would appear a priori that there is little basis for it being a good proxy of phytoplankton carbon. In essence, to provide a useful proxy of phytoplankton carbon, the scattering methods must fulfill the following condition for the time and space scales of interest: the variability in c_p or b_{bp} due to changes in phytoplankton biomass (average cellular carbon content times cell number) must be “much” higher than variability in c_p or b_{bp}

BGD

4, 707–745, 2007

Proxies of biomass for primary production

Y. Huot et al.

Title Page

Abstract

Introduction

Conclusions

References

Tables

Figures

◀

▶

◀

▶

Back

Close

Full Screen / Esc

Printer-friendly Version

Interactive Discussion

EGU

due to changes in non-phytoplanktonic particle type and size distribution, or they must be highly correlated. We will examine here both b_{bp} and c_p (approximated as b_b) as potential alternatives to Tchl_a for the estimate of photosynthetic parameters.

Another proxy examined herein is phytoplankton absorption (\bar{a}_{phy} , m^{-1}). Indeed despite methodological problems linked to its determination, it has sometimes been argued that \bar{a}_{phy} is preferable to Tchl_a for studies of primary productivity (Perry, 1994; Lee et al., 1996; Marra et al., 2007). The basis for this proposition is that \bar{a}_{phy} is more directly linked the remote sensing signal and photosynthetic processes than Tchl_a (Perry, 1994). The evidence for this suggestion is, however, still lacking on large oceanic scales.

Other potentially useful measures examined in this paper are the: photosynthetic absorption (\bar{a}_{ps} , m^{-1}) which encompasses all and only the photosynthetic pigments; chlorophyll a fluorescence, which is due to the absorption by all photosynthetic pigments and has the advantage of being readily measured in the ocean with high temporal and spatial resolution but is strongly affected by the physiological state of the algae; and picophytoplankton biovolume obtained by flow cytometry.

The approach followed will be to use straightforward analyses to verify if any of these proxies can be effectively substituted for Tchl_a to obtain more precise information about the phytoplankton photosynthetic parameters. For this study, we will use a dataset obtained during the BIOSOPE cruise. This cruise encompassed a large range of trophic conditions from the hyperoligotrophic waters of the South Pacific Gyre to the eutrophic conditions associated with the Chile upwelling region, also investigating the mesotrophic HNLC (high nutrient low chlorophyll) waters of the subequatorial region and in the vicinity of the Marquesas Islands. It is thus expected that the conclusions reached by our analysis can be extrapolated with some confidence to other open ocean waters. This is tested here by comparing our results with those obtained during the PROSPE cruise which sampled the Moroccan upwelling and the Mediterranean sea. Firstly, we will compare P_{max} and α to the different proxies to assess which measure is most accurate when taken alone to estimate photosynthetic biomass. Sec-

BGD

4, 707–745, 2007

Proxies of biomass for primary production

Y. Huot et al.

Title Page

Abstract

Introduction

Conclusions

References

Tables

Figures

◀

▶

◀

▶

Back

Close

Full Screen / Esc

Printer-friendly Version

Interactive Discussion

EGU

only, we attempt to explain the remaining variability in terms of simple oceanographic variables with our aim being to understand which proxy of phytoplankton biomass provides the most accurate predictions of photosynthetic parameters when additional data is available.

2 Background

As mentioned in the introduction, equations 3 and 5 provide a good start for evaluating potential biomass estimators of photosynthetic parameters. These equations show that photosynthetic parameters that are not normalized to biomass can in fact be considered a proxy of photosynthetic biomass. That is, at the first order, they represent the part of the phytoplankton biomass (not necessarily in carbon units) that leads to photosynthesis, though tainted by physiological variability (the same is, however, true of all other biomass proxies which are not phytoplankton carbon per se). The advantage of the photosynthetic parameters, used as a proxy of photosynthetic biomass, is that they are specific to primary producers and can be measured on bulk samples. Furthermore, the relatively constant value of P_{\max} when normalized to phytoplankton carbon observed in cultures (MacIntyre et al., 2002) suggests that P_{\max} may be a good proxy of phytoplankton carbon (though interspecific variability can be large). The P_{\max} and α are, however, related to two different biomass measures, one reflecting the algal capacity to utilize low irradiance (\bar{a}_{ps}) and one reflecting their maximal capacity to utilize saturating irradiance (n_{slowest}).

Normalization of P_{\max} to different proxies of phytoplankton biomass (B) leads to $P_{\max}^B = 7.174 \times 10^{-17} \frac{n_{\text{slowest}}}{B} \frac{1}{\bar{\tau}_{\text{slowest}}}$, and the same normalization for α leads to $\alpha^B = 43.2 \frac{\bar{a}_{ps}}{B} \varphi_{C \max}^{ps}$. Since the variability in $\varphi_{C \max}^{ps}$ and $\bar{\tau}_{\text{slowest}}$ is not a priori related to B (though it may be at second order in situ through covariation with community structure), normalization by B attempts to remove the variability in P_{\max} and α originating from changes in biomass. Any proxy of biomass that covaries with \bar{a}_{ps} and n_{slowest} will

BGD

4, 707–745, 2007

Proxies of biomass for primary production

Y. Huot et al.

Title Page

Abstract

Introduction

Conclusions

References

Tables

Figures

◀

▶

◀

▶

Back

Close

Full Screen / Esc

Printer-friendly Version

Interactive Discussion

EGU

Proxies of biomass for primary production

Y. Huot et al.

Title Page

Abstract

Introduction

Conclusions

References

Tables

Figures

◀

▶

◀

▶

Back

Close

Full Screen / Esc

Printer-friendly Version

Interactive Discussion

remove some of the variability, but proxies that are better correlated (thus accounting for more of the sources of variability) will perform best. For example, normalizing α by $\bar{\alpha}_{\text{phy}}$ does not account for the variability in the ratio of photosynthetic absorption to total phytoplankton absorption, while normalizing by Tchl_a leaves the variability in the photosynthetic absorption to Tchl_a. Thus, while “most” of variability caused by changes in biomass is accounted for by the normalization, some variability is left. Furthermore, sources of variability that were not originally present can be added by an inappropriate normalization. It follows that, while there are good arguments for working on the biomass normalized photosynthetic parameters (e.g. Platt and Sathyendranath, 1999), it also makes sense to work directly on the parameters from a predictive perspective, as prediction of the “added” variability is unnecessary. This is the approach that will be followed herein. Table 1 describes the different sources of variability that are not accounted for when a given biomass proxy is used to normalize the photosynthetic parameters. To aid in the interpretation of our results, and to elaborate on Table 1, we address in more detail here the case of the scattering and backscattering coefficients.

The particulate scattering coefficient is the sum of scattering by all particles. The relative contribution of each particle type depends on their scattering efficiency (which depends on their size, shape, structure, and index of refraction) and on their concentration (Morel, 1973; Morel and Bricaud, 1986). Given a Junge particle distribution of homogenous spherical particles, those in the size range of 0.5 to 20 μm (Morel, 1973) will be the most effective at scattering. In the ocean, we can express the particulate scattering coefficient as:

$$b_p = b_{\text{phy}} + b_{\text{bact}} + b_{\text{het}} + b_{\text{vir}} + b_{\text{min}} + b_{\text{bub}} + b_{\text{org}},$$

where b_{phy} , b_{bact} , b_{het} , b_{vir} , b_{min} , b_{bub} , b_{org} are the contributions from phytoplankton, bacteria, small non-bacterial heterotrophs, viruses, mineral non-phytoplanktonic particles, bubbles, and non-living organic matter, respectively. We can thus express the

scattering normalized P_{\max} as:

$$P_{\max}^{b_p} = 7.174 \times 10^{-17} \left(\frac{n_{\text{slowest}}}{b_{\text{phy}}} \right) \left(\frac{b_{\text{phy}}}{b_{\text{phy}} + b_{\text{bact}} + b_{\text{het}} + b_{\text{vir}} + b_{\text{min}} + b_{\text{bub}} + b_{\text{org}}} \right) \frac{1}{\bar{\tau}_{\text{slowest}}}$$

a similar equation is obtained for α :

$$\alpha^B = 43.2 \left(\frac{\bar{a}_{ps}}{b_{\text{phy}}} \right) \left(\frac{b_{\text{phy}}}{b_{\text{phy}} + b_{\text{bact}} + b_{\text{het}} + b_{\text{vir}} + b_{\text{min}} + b_{\text{bub}} + b_{\text{org}}} \right) \varphi_{C_{\max}}^{ps}$$

- 5 Therefore, b_p provides a good biomass proxy for normalizing the photosynthetic parameters if b_{phy} is a good proxy for n_{slowest} or \bar{a}_{ps} (i.e. low natural variability within the first parentheses of the equations above) and if, in addition, it meets one of three requirements (low variability in the second parentheses): 1) b_p must be mostly influenced by b_{phy} and all other constituents must represent small or negligible contributions to scattering; 2) all other constituents' scattering coefficients must covary tightly with b_{phy} ; or 3) a combination of the first two conditions leading to a reduced variability in the b_{phy} to b_p ratio.

15 Measurements of particulate scattering in the ocean are always derived from measurements of attenuation by subtracting the attenuation by water and the total absorption ($b_p = c_p - a_{\text{tot}}$). When absorption is small relative to scattering, c_p is approximately equal to b_p . This applies to case 1 waters for the wavebands near 660 nm (Loisel and Morel, 1998).

20 Theoretically, particulate backscattering is due to the same constituents as scattering, but the efficiency of backscattering is more strongly weighted towards smaller sized particles (~ 0.1 to $1 \mu\text{m}$ c.f., Morel and Ahn, 1991). Alternatively, it can be due to structure within larger cells leading to a greater backscattering efficiency compared to standard calculation made with uniform spheres. To be a good proxy of photosynthetic biomass, b_{bp} must meet the same three conditions mentioned above for b_p .

BGD

4, 707–745, 2007

Proxies of biomass for primary production

Y. Huot et al.

Title Page

Abstract

Introduction

Conclusions

References

Tables

Figures

◀

▶

◀

▶

Back

Close

Full Screen / Esc

Printer-friendly Version

Interactive Discussion

EGU

3 Materials and methods

All of the data presented herein were collected during the BIOSOPE and PROSOPE cruises. BIOSOPE sampled 2 transects from the Marquesas Islands to Easter Island, and from Easter Island to Concepcion Chile, through the South Pacific Gyre from 26 October to 10 December 2004. PROSOPE sampled the Morocco upwelling and the Mediterranean Sea from 4 September to 4 October 1999 (see Oubelkheir et al., 2005 for cruise track). Because the dataset for the BIOSOPE cruise is more complete and allows consistent analyses between the parameters studied, we carried out the statistical analysis on that dataset only, and use the PROSOPE dataset for comparison purposes only. While we will not discuss the comparison with the PROSOPE dataset further, we will mention here that trends and absolute values compare well with the BIOSOPE dataset for all variables. All the data shown here are obtained from CTD and rosette casts made near solar noon. Nine depths were usually sampled for the PvsE experiments and all data are matched to these depths. For discrete samples obtained from Niskin bottles (e.g. Tchl_a, PvsE parameters and absorption), we compare data from the same bottle or from duplicate bottles from the same depth as the PvsE curve data. The data obtained from profiling instruments (e.g. CTD, fluorescence, b_p and b_{bp}), are from the same cast as that of the PvsE sample, and represent the average over 2 m centered on the depth of the PvsE bottle.

3.1 Photosynthesis vs. irradiance curves

The PvsE curves of the particulate fraction were determined by closely following the protocol of Babin et al. (1994). One modification was made for the BIOSOPE cruise (but not PROSOPE): we replaced the GFF filters with 0.2 μm pore size polycarbonate membrane filters. This modification reduced the dispersion observed in surface samples (M. Babin, personal observation). Incubations lasted between 2 and 3.5 h. The data were fit to Eq. (2). The P_{max} reported are equal to $P_{\text{max}} + P_o$ (e.g. MacIntyre and Cullen, 2005). The 95% confidence interval (CI) on the parameters was estimated

BGD

4, 707–745, 2007

Proxies of biomass for primary production

Y. Huot et al.

Title Page

Abstract

Introduction

Conclusions

References

Tables

Figures

◀

▶

◀

▶

Back

Close

Full Screen / Esc

Printer-friendly Version

Interactive Discussion

EGU

using the standard MATLAB routine *nlpredci.m*. Estimated parameters for which the CI were greater than 50% of the parameter value were discarded. To have a uniform dataset, we also discarded the points for which there were no concurrent values for all of the following: Tchl_a, b_p , b_{bp} , a_{phy} , a_{ps} , and nitrate. This left 167 points for P_{max} and 159 points for α from an original dataset of 338 PvsE curves. Roughly half of the points we removed (77 for P_{max} and 75 for α) were excluded because of the criteria we chose for the CI. Since the number of phytoplankton biovolume estimates was significantly smaller, data for missing biovolume estimates were not excluded.

3.2 Pigments

The concentration of phytoplankton pigments was measured by HPLC, using a method modified from the protocol of Van Heukelem and Thomas (2001) for the BIOSOPE cruise (Ras et al., 2007¹), and Vidussi et al. (1996) for the PROSOPE cruise.

3.3 Phytoplankton and photosynthetic absorption

The method used for phytoplankton absorption spectra measurements is detailed in the works of Bricaud et al. (1998) and Bricaud et al. (2004). Photosynthetic absorption was obtained following the procedure of Babin et al. (1996) using the individual pigment spectra in solution given by Bricaud et al. (2004). Both were weighted according to the irradiance inside the photosynthesetron (see Eq. 4; the same equation was used for \bar{a}_{phy} by replacing a_{ps} by a_{phy}) to provide an average value for the spectra.

3.4 Fluorescence

Fluorescence was measured in situ using an Aquatracka III fluorometer (Chelsea Technology Group) placed on the same rosette as the Niskin bottle for the discrete samples.

¹Ras, J., Uitz, J., and Claustre, H.: Spatial variability of phytoplankton pigment distribution in the South East Pacific, in preparation, 2007.

BGD

4, 707–745, 2007

Proxies of biomass for primary production

Y. Huot et al.

Title Page

Abstract

Introduction

Conclusions

References

Tables

Figures

◀

▶

◀

▶

Back

Close

Full Screen / Esc

Printer-friendly Version

Interactive Discussion

EGU

3.5 Scattering and backscattering coefficient

The scattering and backscattering coefficients were measured using an AC-9 (WET Labs) and an ECO-BB3 sensor (WET Labs), respectively. AC-9 data was acquired and processed according to the method of Twardowski et al. (1999), using the temperature and salinity correction coefficients obtained by Sullivan et al. (2006). Scattering errors in the reflective tube absorption measurement were corrected using the spectral proportional method of Zaneveld et al. (1994). Between field calibrations with purified water during the cruise, instrument drift was fine-tuned to independent measurements of absorption in the dissolved fraction made on discretely collected samples by (Bricaud et al., 2007²). The ECO-BB3 data were processed according to Sullivan et al. (2005), using the chi-factors obtained therein to convert volume scattering measurements at 117 degrees to backscattering coefficients. For optimal accuracy, direct measurements of in situ dark counts were periodically collected by placing black tape over the detectors for an entire cast.

3.6 Diffuse attenuation coefficient

The diffuse attenuation coefficient (K_d , m^{-1}) in the visible bands was obtained as described in Morel et al. (2007).

3.7 Phytoplankton biovolumes

Prochlorococcus, *Synechococcus* and picophytoeukaryote biovolumes were estimated from mean cell size and abundance by assuming a spherical shape, see Grob et al. (2007)³ for details. Cell abundances were directly determined using flow cytometry,

²Bricaud, A., Babin, M., Claustre, H., Ras, J., and Tieche, F.: The partitioning of light absorption in South Pacific Waters, in preparation, 2007.

³Grob, C. Ulloa, O., Claustre, H., Huot, Y., Alarcon, G., and Marie, D.: Contribution of picoplankton to the particulate attenuation coefficient (cp) and organic carbon concentration

BGD

4, 707–745, 2007

Proxies of biomass for primary production

Y. Huot et al.

Title Page

Abstract

Introduction

Conclusions

References

Tables

Figures

◀

▶

◀

▶

Back

Close

Full Screen / Esc

Printer-friendly Version

Interactive Discussion

EGU

Proxies of biomass for primary production

Y. Huot et al.

Title Page

Abstract

Introduction

Conclusions

References

Tables

Figures

◀

▶

◀

▶

Back

Close

Full Screen / Esc

Printer-friendly Version

Interactive Discussion

except for the weakly fluorescent surface *Prochlorococcus* populations whose abundance was estimated from divinyl chlorophyll *a* concentrations. Mean cell sizes were obtained by establishing a direct relationship between the cytometric forward scatter signal (FSC) normalized to reference beads and cell size measured with a Coulter Counter for picophytoplanktonic populations isolated in situ and cells from culture (see Sect. 2.1 and Fig. 3a in Grob et al., 2007³). Mean cell sizes were then used to calculate cell volumes assuming a spherical shape. Finally, biovolumes ($\mu\text{m}^3 \text{ ml}^{-1}$) were obtained by multiplying cell volume and abundance. Because, as noted above, in surfaces water at some stations, the *Prochlorococcus* population fluorescence was too low to detect, we discarded all *Prochlorococcus* measurements for this study. The biovolumes thus include only the *Synechococcus* and picophytoeukaryotes. The maximum cell diameter observed with the instrument settings used during the cruise was $3 \mu\text{m}$, this included most of the phytoplankton cells in oligotrophic waters but missed a significant fraction in more eutrophic waters.

3.8 Stepwise regression and determining the quality of fits

We use three quantities to assess the quality of fits: the correlation coefficient (r), the root mean square error (RMSE), and the mean absolute percent error (MAPE). While the first two are more commonly used statistical measures of fits, the third provides an estimate of variability that is independent of range or absolute values (relative measure, without units) of the data and hence is more easily comparable between different estimated variables. The MAPE is expressed as a fraction (instead of a percentage, sometimes abbreviated as MAE in the literature) and is calculated as $\text{MAPE} = \frac{1}{n} \sum_{i=1}^n \left(Y_i - \hat{Y}_i \right) / Y_i$, where Y is the measured data, \hat{Y} is the estimated value and n the total number of points.

All stepwise regressions will be conducted with the following constraints, a variable (POC) in the eastern South Pacific, in preparation, 2007.

is added if the maximum p-value is 0.05 and removed if the minimum p-value is 0.10. The p-values provided in the text regarding the stepwise regression are the probability that the regression coefficient is equal to 0.

4 Results and discussion

4.1 Overview of the dataset

An overview of the biomass data collected during the BIOSOPE cruise shows that most variables follow the trends expected as a function of chlorophyll *a* for case 1 waters (Fig. 1). Indeed, relationships between surface measurements of b_p , b_{bp} , and a_{phy} and Tchl a concentration are consistent with statistical relationships previously established for case 1 waters. It is interesting to note the resemblance between panels *A* and *H* showing respectively b_p and the phytoplankton biovolume obtained from the flow cytometry measurements as a function of the Tchl a concentration. The decrease of b_p with depth for a given Tchl a concentration (Fig. 1a) is also consistent with the oft-reported trends attributed to a “photoacclimation-like” behavior (i.e.. an increase in the Tchl a per scattering particle, c.f. Behrenfeld and Boss 2006 and references therein). A similar trend is observed in b_{bp} (Fig. 1b). The phytoplankton absorption (Fig. 1c) generally follows the statistical relationship established for case 1 waters by Bricaud et al. (2004) but shows a slightly higher slope and lower intercept. A sigmoidal shape is observed in log space for the fluorescence vs Tchl a relationship (Fig. 1d). A clear depth dependence is observed in the P_{max} vs Tchl a relationship, while this dependence is reversed and seems less accentuated for α (Figs. 1e and f, note that our quality control rejected many deep estimates of α ; see Methods section). The relationship between α and P_{max} (Fig. 1g) also shows a depth dependence which represents changes in E_k with depth (i.e. higher values at the surface; lower values at depth).

A comparison of the distribution of the photosynthetic parameters when they are normalized by Tchl a or by the particulate scattering coefficient is provided in Fig. 2.

Title Page

Abstract

Introduction

Conclusions

References

Tables

Figures

◀

▶

◀

▶

Back

Close

Full Screen / Esc

Printer-friendly Version

Interactive Discussion

Proxies of biomass for primary production

Y. Huot et al.

Title Page

Abstract

Introduction

Conclusions

References

Tables

Figures

◀

▶

◀

▶

Back

Close

Full Screen / Esc

Printer-friendly Version

Interactive Discussion

The values obtained for P_{\max}^{chl} (0.26 to 7.2 mg C mg chl m⁻³ h⁻¹) and α^{chl} (0.0028 to 0.086 mg C mg chl m⁻³ h⁻¹ ($\mu\text{mol photons m}^{-2} \text{s}^{-1}$)⁻¹) are consistent with values from the literature, but clearly do not cover the full range of variability reported. A review of several datasets of photosynthetic parameters by Behrenfeld et al. (2004) gives a range of 0.04 to 24.3 (mostly between ~ 0.5 and ~ 10) mg C mg chl m⁻³ h⁻¹ for P_{\max}^{chl} , and of 0.0004 to ~ 0.7 (mostly between ~ 0.005 and ~ 0.2) mg C mg chl m⁻³ h⁻¹ ($\mu\text{mol photons m}^{-2} \text{s}^{-1}$) for α^{chl} though some variability in α^{chl} originates from a different spectrum used for the measurement of irradiance. Using a crude index of dispersion, the normalized range (see Figure 2 caption for details), shows that normalization of both P_{\max} and α by Tchl_a reduces the variability in the data relative to normalization by b_p (but only slightly in the case of P_{\max}). The distribution for P_{\max} normalized to b_p , however, shows a normal distribution of points below values of 7 mg C mg chl m⁻³ h⁻¹ with a long tail above. If we consider only the points below 7, the variability is much reduced and becomes lower than when Tchl_a is used as the normalization factor (even excluding the point above $P_{\max}^{\text{chl}}=6$). The higher P_{\max} normalized to b_p values occur mostly in regions with higher chlorophyll concentrations (coastal upwelling regions, deep chlorophyll maxima, and Marquesas Islands), which could be real, or indicate a bias in the normalization by b_p with trophic status (e.g. ratio of b_{phy}/b_p increasing with increasing chlorophyll concentration due to changing particle composition and size distribution, see Table 1 and Background section).

4.2 Determining the best proxy of phytoplankton biomass to predict photosynthetic parameters

Figure 3 shows the comparison between P_{\max} and different measures of biomass. The left panels show the scatter plots of P_{\max} against the different biomass indices measured, and a 2nd order polynomial obtained on the log-transformed data. The right-hand-side panels show the values of P_{\max} predicted by using the polynomial fit against the measured values (the statistics of the fits are also provided). As previously men-

tioned, all fits and statistics refer only to the BIOSOPE dataset as it is more complete and allows a consistent comparison of all proxies of biomass from an equal number of points taken simultaneously, or near simultaneously, while the PROSOPE dataset is superposed for comparative purposes only. Several points can be made about this figure. Firstly, the $b_p(650)$ and biovolumes estimated from flow cytometry measurements provide the best estimates of P_{\max} . Since the variability in $\bar{\tau}_{\text{slowest}}$ and the measurement errors on P_{\max} are equal for all panels, this suggests that $b_p(650)$ is the best single measure of n_{slowest} . Secondly, the backscattering coefficient provides estimates of P_{\max} that are equivalent to those using Tchl_a. However, at low values of P_{\max} the predictability is reduced as the slope between P_{\max} and b_{bp} is much smaller. Indeed, for values of $P_{\max} < \sim 0.1$, b_{bp} continues to decrease while P_{\max} remains constant. In these waters with low concentrations of particulate matter, b_{bp} is particularly difficult to measure given the low signal available to in situ instruments. Thirdly, a_{ps} , a_{phy} and chlorophyll fluorescence all perform similarly in estimating P_{\max} but slightly worse than Tchl_a. We can summarize these results in terms of decreasing accuracy of estimates (using MAPE as the index) as follows: $b_p \approx \text{biovolume} > \text{Tchl}_a \approx b_{bp}(650) \approx \text{fluo} \approx a_{phy} \approx a_{ps}$. Statistically, the correlation coefficient (r) on b_p is significantly greater ($p < 0.05$, t-test on the z-transform of the correlation coefficient, Sokal and Rohlf, 1995) than the parameters with values of r equal to or lower than that of Tchl_a (i.e. Tchl_a, $b_{bp}(650)$, fluorescence, a_{phy} , a_{ps}). There is no significant difference between the correlation coefficients on the other parameters.

Figure 4 shows the comparison between α and different measures of biomass. In contrast with the P_{\max} measurements, both measures of scattering as well as the biovolume estimates perform very poorly, while Tchl_a and \bar{a}_{ps} show the best estimates, with Tchl_a outperforming \bar{a}_{ps} only very slightly. Finally, fluorescence is followed by \bar{a}_{phy} . In summary, estimators order as follows (from the most to the least accurate): Tchl_a $\approx \bar{a}_{ps} \approx \text{fluo} > \bar{a}_{phy} \gg b_p > \text{biovolumes} > b_{bp}$. Statistically, the correlation coefficient of Tchl_a is significantly greater than the other proxies with values of r equal or lower to that of a_{phy} ($p < 0.05$; t-test on z-transform). The correlation coefficient on \bar{a}_{phy} is signif-

Proxies of biomass
for primary
production

Y. Huot et al.

Title Page

Abstract

Introduction

Conclusions

References

Tables

Figures

◀

▶

◀

▶

Back

Close

Full Screen / Esc

Printer-friendly Version

Interactive Discussion

icantly different from b_p , b_{bp} or biovolumes ($p < 0.001$; t-test on the z-transform). Other significant differences (e.g. between fluorescence and b_{bp}) exist but are not important in this context. The difference between \bar{a}_{ps} and \bar{a}_{phy} is not significant ($p = 0.12$).

To summarize these results, it can be said that we obtained very intuitive results for the relationships between α and the different proxies of photosynthetic biomass. Indeed, that Tchl a , \bar{a}_{ps} , and \bar{a}_{phy} provide the best measures of α is what we expected as they represent a measure closely related to the absorption of photosynthetic pigments. On the other hand, the results concerning P_{max} are more surprising: b_p , despite not being specific to phytoplankton, provides a better estimate of P_{max} than the traditional measure of Tchl a . Hence, for the waters studied here, which are representative of many oceanic waters, b_p is the best proxy for estimating P_{max} when no other measurements are available. This means that b_p is strongly influenced by phytoplankton scattering or that the scattering coefficients of all other particulate matter show tight relationships with the phytoplankton scattering coefficient. Furthermore, since it is better correlated to P_{max} than Tchl a , which is present only in phytoplankton, it implies that b_p provides a measure that covaries better with $n_{slowest}$ than Tchl a . Consequently, it also means that there is considerable variability in the ratio $n_{slowest}/Tchl_a$ (not correlated with Tchl a). Even more surprising is the good retrieval of P_{max} using $b_{bp}(650)$ which is equivalent to estimates using Tchl a . Because the size fractions that are expected to influence b_{bp} the most are smaller than the smallest phytoplankton (assuming a Junge distribution, generally observed during BIOSOPE, Sciandra et al., 2007⁴), it implies that either backscattering from that fraction is very well correlated with phytoplankton backscattering, or that organelles within phytoplankton cells are affecting b_{bp} . Actually, phytoplankton are not spheres of uniform refractive index and more elaborate models may be more appropriate (e.g. Kitchen and Zaneveld, 1992); Mie calculation may underestimate their contribution to oceanic scattering.

⁴Sciandra, A., Stramski, D., and Babin, M.: Variability in particle size distribution in contrasted trophic regions of the South East Pacific, in preparation, 2007.

**Proxies of biomass
for primary
production**

Y. Huot et al.

Title Page

Abstract

Introduction

Conclusions

References

Tables

Figures

◀

▶

◀

▶

Back

Close

Full Screen / Esc

Printer-friendly Version

Interactive Discussion

4.3 Using environmental variables in addition to proxies of phytoplankton biomass

While the results of the previous analysis are interesting, it remains a somewhat academic exercise because biomass proxies are rarely obtained without at least some information about the sampled location and environment. We thus, now turn to our second question. Can we improve the estimates of α and P_{\max} by using additional measurable quantities? In other words, what is the origin of the remaining variability?

To address this question we used a stepwise regression analysis with the log transform of α and P_{\max} as our dependent variable and a series of potentially relevant independent variables. For each fit, we used only one log-transformed “biomass proxy” (i.e. whether $\log(\text{Tchl}a)$, $\log(b_p)$, $\log(b_{bp})$...). The analysis was conducted for all depths. Table 2 provides all the independent variables tested and a summary of the results.

Figure 5 compares graphically the results for P_{\max} using $b_p(650)$ and $\text{Tchl}a$ as the independent biomass variable.

The results are clear (see Table 2, e.g. MAPE row). Using other independent variables beyond biomass, it is possible to significantly improve the relationship between P_{\max} and $\text{Tchl}a$ (as well as a_{phy} , a_{PS} , and fluorescence). However, the same does not occur for b_p or b_{bp} , for which the relationships improve only marginally by using several new variables. Most of the improvements using $\text{Tchl}a$ arise from accounting for the depth effects. This is not unexpected given the clear depth dependence of P_{\max} for a given $\text{Tchl}a$ concentration observed in Fig. 1e. The relationships retrieved or the parameters used are not discussed further here, but the result that interests us is that the pigment or absorption based estimates of P_{\max} can be relatively easily improved beyond a simple biomass relationship whereas the same is not true for the scattering based methods. The latter hence have lower predictive skill when other sources of variability are accounted for. We also note that the errors on the prediction of P_{\max} using our simple regression approach with $\text{Tchl}a$ are very reasonable; the average error (MAPE) is 25% for the BIOSOPE dataset (see Table 2) and 33% for the independent

BGD

4, 707–745, 2007

Proxies of biomass for primary production

Y. Huot et al.

Title Page

Abstract

Introduction

Conclusions

References

Tables

Figures

◀

▶

◀

▶

Back

Close

Full Screen / Esc

Printer-friendly Version

Interactive Discussion

EGU

PROSOPE dataset.

We carried out a similar analysis for α (Table 3 and Fig. 6). In this case, all estimates improved by important margins relative to the relationship using only the biomass index. However, the Tchl_a and absorption based measures remained significantly better than the scattering based methods (Table 3). In fact, the improvements in the scattering based methods are due to the fact that they started off so poorly, and any variable that is somewhat correlated with α will improve the relationships.

4.4 Further considerations in the context of remote sensing applications

In summary, simple functions of Tchl_a along with information about the irradiance or depth appear more accurate for estimating photosynthetic parameters (and eventually primary productivity) than scattering based methods. This is true for in situ sampling and for BIOSOPE waters probably representative of many open ocean conditions. Using remote sensing data, additional errors inherent to the determination of the biomass proxies must be taken into account.

Of the variables tested here, two can be estimated from ocean color remote sensing due to their direct effect on the upwelling radiance: phytoplankton absorption and total backscattering. Retrievals of chlorophyll *a* rely on the fact that it covaries strongly with these two variables. In the same way, algorithms can be described to obtain the total scattering or beam attenuation coefficients (Roesler, 2003; Doron et al., 2007), but they rely on more or less robust empirical relationships rather than on a direct effect on the upwelling radiance and, thus, would include more errors than the backscattering measurements. Therefore, unless the estimate of the backscattering coefficient from remote sensing is much more accurate than that of phytoplankton absorption or chlorophyll *a*, there is little opportunity to improve the determination of photosynthetic biomass from space using scattering or backscattering based algorithms. However, estimates of the backscattering coefficient tend indeed to be more accurate than those of Tchl_a from remote sensing. To test the possibility that backscattering could improve estimates of photosynthetic biomass at light saturation, we conducted the same anal-

BGD

4, 707–745, 2007

Proxies of biomass for primary production

Y. Huot et al.

Title Page

Abstract

Introduction

Conclusions

References

Tables

Figures

◀

▶

◀

▶

Back

Close

Full Screen / Esc

Printer-friendly Version

Interactive Discussion

EGU

ysis by stepwise regression as previously done for P_{\max} but restricted the depth range to the first optical depth at 490 nm (obtained as $1/K_d(490)$, leaving 45 points). We thus obtained two regression equations for the estimate of P_{\max} using Tchl a or b_{bp} as the phytoplankton biomass proxy. From these equations, we can use standard theory for the propagation of errors to test if we can obtain lower dispersion using the backscattering coefficient. This analysis is presented in Appendix A, and shows that for realistic values of the error on backscattering and Tchl a , it is not possible to improve estimates of the photosynthetic parameters for the BIOSOPE region in the context of the regression equations developed here.

4.5 Additional information in the scattering based measurements beyond Tchl a

An important question remains: given the regression using Tchl a , can scattering based variables allow us to improve estimates of P_{\max} and α ? In other words, is there supplementary information in the scattering based proxies? This question can also be addressed by a stepwise regression analysis, by verifying if adding scattering based measures improves the fit significantly. We tested the addition of the following variables: $b_p(650)$, $b_p(650)^2$, and Tchl $a/b_p(650)$. None of them provided significant improvements in the regression of P_{\max} (all had values of $p > 0.17$) or α (all had values of $p > 0.14$). We therefore conclude that, for the waters studied, which are probably representative of many open ocean waters, bulk scattering measurements cannot be used to improve estimates of photosynthetic biomass (or parameters), once basic information regarding chlorophyll concentration and irradiance at depth is available (see Tables 2 and 3).

This conclusion is of course only valid for the environments and the space and time scales that we studied. Scattering based measurements have been proposed to help in the estimation of primary production based on diurnal changes in the c_p (e.g. Siegel et al., 1989) or of phytoplankton carbon concentration and growth rate from space on large spatial scales (Behrenfeld et al., 2005). These applications are beyond the scope of our analysis and our results are difficult to extrapolate to them. Our results,

**Proxies of biomass
for primary
production**

Y. Huot et al.

Title Page

Abstract

Introduction

Conclusions

References

Tables

Figures

◀

▶

◀

▶

Back

Close

Full Screen / Esc

Printer-friendly Version

Interactive Discussion

however, suggest that, if P_{\max} is a good proxy for phytoplankton carbon as mentioned previously, better estimates of phytoplankton carbon may be obtained by functions of Tchl_a and other variables rather than scattering based algorithms on certain time and space scales.

5 4.6 Further considerations in view of modeling the global primary productivity

We will, digress here from our strict appraisal of the photosynthetic parameters to examine one particular aspect of the estimation of phytoplankton carbon using backscattering with our dataset. In particular, we want to return to the functional relationship retrieved by Behrenfeld et al. (2005) between the chlorophyll *a* concentration and b_{bp} (Fig. 1b in the present work; Fig. 1 in Behrenfeld et al., 2005). This relationship deserves particular consideration as it forms the basis of their carbon-based model of primary productivity, growth rate and physiology from space. It was obtained by comparing chlorophyll *a* and backscattering obtained for large predefined regions using remotely sensed estimates of surface chlorophyll, based on the model of Maritorena et al. (2002). Apart from a significant difference in the absolute values retrieved at a given chlorophyll concentration for which there is no obvious explanation, their relationship shows another important departure from our data. According to Behrenfeld et al. (2005), the values of b_{bp} remain quasi-constant in the low chlorophyll *a* domain (i.e. 0.03–0.14 mg m⁻³). By contrast, this “plateau” is not observed in the BIOSOPE dataset (Fig. 1b). Behrenfeld et al. (2005), assuming that a simple function of b_{bp} provided a good proxy of phytoplankton carbon biomass, interpreted the plateau as originating from variability in the intracellular chlorophyll concentration, which would allow variation in chlorophyll *a* but not in backscattering (same number and size of cells). Reconciling our relationship with theirs requires either 1) that the intracellular variability occurs mostly on large time and space scales, but is not observed at the small scales sampled during the BIOSOPE cruise, or 2) that our study area shows different behaviors from a global dataset. Neither explanation seems reasonable to

Proxies of biomass for primary production

Y. Huot et al.

Title Page

Abstract

Introduction

Conclusions

References

Tables

Figures

◀

▶

◀

▶

Back

Close

Full Screen / Esc

Printer-friendly Version

Interactive Discussion

**Proxies of biomass
for primary
production**

Y. Huot et al.

 Title Page

Abstract

Introduction

Conclusions

References

Tables

Figures

◀

▶

◀

▶

Back

Close

Full Screen / Esc

Printer-friendly Version

Interactive Discussion

us. While the first point cannot be completely rejected, the second one can given on the good correspondence of the BIOSOPE dataset with the best estimates in the literature for case 1 waters (Morel and Maritorena, 2001). We observe, however, that the plateau found by Behrenfeld et al. (2005) corresponds to a similar plateau (actually low accuracy in retrieval) observed by Maritorena et al. (2002) on their quasi-real data set below $b_{bp}(443) \sim 0.0015 \text{ m}^{-1}$. While this does not affect the validity of the approach followed by Behrenfeld et al. (2005), we do propose that a possible reason for the plateau is simply a bias in the inversion model. This situation clearly points to a need for further research in regions with low chlorophyll concentration. Since roughly 50% of the world's ocean have chlorophyll values below 0.14 mg (Antoine et al., 2005), correct parameterization below this concentration is critical if global estimates are to be made. Regarding these low-chlorophyll waters, we note that the recent comparison of semi-analytical models using the IOCCG synthetic dataset (IOCCG, 2006) has only 11 out of 500 points below $b_b(470) = 0.001 \text{ m}^{-1}$, and is therefore of little help in resolving this issue; most of the BIOSOPE dataset lies below $b_b(470) = 0.001 \text{ m}^{-1}$.

As mentioned previously, primary productivity models are generally expressed with the production irradiance relationship normalized to biomass (e.g. P^B). This relationship is depth integrated and then multiplied by biomass, $P = BP^B$. In order to reduce the variability in P^B , some authors try to relate it to its location and time (Longhurst 1998; Platt and Sathyendranath 1999), while others describe it in terms of environmental variables (e.g., $P^B(T, \text{Salinity}, E_d)$) (Behrenfeld and Falkowski, 1997). The aim of our study is to identify the normalization factor (“B”) that reduces as much as possible the variability in the photosynthetic parameters. In doing so, we obtain regressions that predict P_{\max} and α for different biomass proxies and environmental variables (Tables 2 and 3). Our relationships can thus be written as $P = f(B, T, \text{Salinity}, E_d, z \dots)$. This implies that these relationships, or extensions of them, could be used in primary production models using remote sensing data, but without multiplying the resulting primary production by an estimate of the phytoplankton biomass. Here, the phytoplankton biomass serves directly as a predictive variable.

5 Conclusions

Within the context of evolving ocean observation technology, our analysis consolidate a rationale for the direction taken over the past 50 years or so for estimating primary productivity. Indeed, we find that chlorophyll *a* remains the best proxy of phytoplankton biomass for studies of primary productivity. In particular, we find that the scattering coefficient (and other scattering-based variables) did not provide information about the photosynthetic parameters that could not be more accurately estimated by a measure of chlorophyll *a* (or fluorescence) and incident irradiance at depth. This is probably due as much to the superior accuracy of the estimation of *Tchl_a* compared to other measurements as to its specificity to phytoplankton. There is one main limitation in our present study: most of our dataset originates from subtropical stratified waters (BIOSOPE) and warm temperate waters (PROSOPE). Photosynthetic parameters depend on environmental variables and thus on the regions sampled. While our measurements are representative of a wide range of chlorophyll concentrations (from ~ 0.02 to $\sim 3 \text{ mg m}^{-3}$) they are thus not representative, for example, of polar or cold temperate water columns or coastal zones. It is possible that in these waters scattering-based algorithms will prove to be more robust for the determination of phytoplankton photosynthetic parameters.

Appendix A

Analysis of the propagation of errors for remote sensing applications

Ocean color remote sensing provides information only about the first optical depth (Gordon and McCluney, 1975). We therefore conducted a stepwise regression analysis for the surface layer only by limiting the depth to the first optical depth (which left 45 points). We find the following relationships for P_{max} using *Tchl_a* as the biomass proxy

BGD

4, 707–745, 2007

Proxies of biomass for primary production

Y. Huot et al.

Title Page

Abstract

Introduction

Conclusions

References

Tables

Figures

◀

▶

◀

▶

Back

Close

Full Screen / Esc

Printer-friendly Version

Interactive Discussion

EGU

$$(r^2=0.96, \text{RMSE}_{\text{pmax}}^{\text{chl}}=0.12, \text{MAPE}=0.22)$$

$$P_{\text{max}}^{\text{chla}} = 2.98 + 0.974 \log_{10} (\text{Tchla}) - 0.259T + 0.00616T^2,$$

and for P_{max} normalized to $b_{bp}(650)$ ($r^2=0.91$, $\text{RMSE}_{\text{pmax}}^{bb}=0.169$, $\text{MAPE}=0.321$)

$$P_{\text{max}}^{bb} = 19.5 + 5.81 \log_{10} [b_b(650)] + 0.726 \log_{10} [b_b(650)]^2 - 0.869T + 0.0203T^2.$$

- 5 To perform the propagation of errors we will assume that the errors on the measurement of the dependent variables in situ (Tchla , b_b and temperature) are small such that all the errors in the relationships ($\text{RMSE}_{\text{pmax}}$) are due to errors from the PvsE measurements and natural variability. We can then write that the expected error on P_{max} from remote sensing will be given by

$$10 \text{RMSE}_{\text{expected}}^X = \sqrt{(\text{RMSE}_{\text{pmax}}^X)^2 + (\text{RMSE}_{\text{RS}}^X)^2},$$

where $\text{RMSE}_{\text{RS}}^X$ is the error on the P_{max} estimate that originates from the remote sensing error on the independent variables and X stands for the biomass estimator chl or b_b .

- 15 If we restrict the error analysis to $z=0$ and further assume that the error on temperature is negligible (adding realistic errors for these parameters has a negligible effect on the results) we have in the case of Tchla:

$$\text{RMSE}_{\text{RS}}^{\text{chl}} = \sqrt{0.949 \text{RMSE}_{\text{chla}}^2}$$

and for backscattering:

$$\text{RMSE}_{\text{RS}}^{bb} = \sqrt{33.8 \text{RMSE}_{bb}^2 + 2.10 \log_{10} [b_b(650)]^2 \text{RMSE}_{bb}^2}.$$

- 20 We can first address a hypothetical case where we have perfect retrieval of $b_b(650)$ from remote sensing ($\text{RMSE}_{bb}=0$) and we find $\text{RMSE}_{\text{expected}}^{bb} = \text{RMSE}_{\text{pmax}}^{bb} = 0.23$. We

BGD

4, 707–745, 2007

Proxies of biomass for primary production

Y. Huot et al.

Title Page

Abstract

Introduction

Conclusions

References

Tables

Figures

◀

▶

◀

▶

Back

Close

Full Screen / Esc

Printer-friendly Version

Interactive Discussion

EGU

find using a typical RMSE error on the chlorophyll concentration of 0.2 (e.g. O'Reilly et al., 1998) that $RMSE_{RS}^{chl} \approx 0.19$ which leads to $RMSE_{expected}^{chl} = 0.23$. Therefore, if estimates of backscattering contain negligible errors, it is possible to obtain estimates of P_{max} that are similar to those using Tchl_a. If, however, we use a realistic (but probably optimistic) value of $RMSE_{bb} = 0.1$ (IOCCG, 2006) we find, for a range of $b_b(650)$ from 0.00012 to 0.002 m^{-1} observed during BIOSOPE, that $0.7 < RMSE_{RS}^{bb} < 0.8$. Therefore, there is little room for improving the estimates of phytoplankton biomass in clear oceanic waters using backscattering given the present day accuracy of backscattering algorithms.

Acknowledgements. D. Tailliez and C. Bournot are warmly thanked for their efficient help in CTD rosette management and data processing. We also want to thank F. Tièche for processing the phytoplankton absorption data, P. Raimbault, J. Ras and A. Morel for providing the nutrient, HPLC and irradiance data. This is a contribution of the BIOSOPE project of the LEFE-CYBER program. This research was funded by the Centre National de la Recherche Scientifique (CNRS), the Institut des Sciences de l'Univers (INSU), the Centre National d'Etudes Spatiales (CNES), the European Space Agency (ESA), The National Aeronautics and Space Administration (NASA) and the Natural Sciences and Engineering Research Council of Canada (NSERC). Y. Huot was funded by postdoctoral scholarships from NSERC (Canada) and CNES (France).

References

- Antoine, D., Morel, A., Gordon, H. R., Banzon, V. F., and Evans, R. H.: Bridging ocean color observations of the 1980s and 2000s in search of long-term trends, *J. Geophys. Res.*, 110, C06009, doi:10.1029/2004JC002620, 2005.
- Babin, M. and Morel, A.: An incubator designed for extensive and sensitive measurements of phytoplankton photosynthetic parameters, *Limnol. Oceanogr.*, 39, 694–702, 1994.
- Babin, M., Morel, A., Claustre, H., Bricaud, A., Kolber, Z., and Falkowski, P. G.: Nitrogen- and irradiance-dependent variations of the maximum quantum yield of carbon fixation in eutrophic, mesotrophic and oligotrophic marine systems, *Deep-Sea Res. Pt. I*, 43, 1241–1272, 1996.

BGD

4, 707–745, 2007

Proxies of biomass for primary production

Y. Huot et al.

Title Page

Abstract

Introduction

Conclusions

References

Tables

Figures

◀

▶

◀

▶

Back

Close

Full Screen / Esc

Printer-friendly Version

Interactive Discussion

EGU

- Behrenfeld, M. J. and Boss, E.; Beam attenuation and chlorophyll concentration as alternative optical indices of phytoplankton biomass, *J. Mar. Res.*, 64, 431–451, 2006.
- Behrenfeld, M. J. and Boss, E.: The Beam attenuation to chlorophyll ratio: An optical index of phytoplankton physiology in the surface ocean?, *Deep Sea Res. part 1*, 50, 1537–1549, 2003.
- Behrenfeld, M. J., Boss, E., Siegel, D. A., and Shea, D. M.: Carbon-based ocean productivity and phytoplankton physiology from space, *Global Biogeochem. Cycles*, 19, GB1006, doi:10.1029/2004GB002299, 2005.
- Behrenfeld, M. J. and Falkowski, P. G.: A consumer's guide to phytoplankton primary productivity models, *Limnol. Oceanogr.* 42, 1479–1491, 1997.
- Behrenfeld, M. J., Maranon, E., D. A., and Hooker, S. B.: Photoacclimation and nutrient-based model of light-saturated photosynthesis for quantifying oceanic primary production, *Mar. Ecol.-Prog. Ser.* 228, 103–117, 2002.
- Behrenfeld, M. J., Prasil, O., Babin, M., and Bruyant, F.: In search of a physiological basis for covariations in light-limited and light-saturated photosynthesis, *J. Phycol.* 40, 4–25, 2004.
- Bricaud, A., Claustre, H., Ras, J., and Oubelkheir, K.: Natural variability of phytoplankton absorption in oceanic waters: influence of the size structure of algal populations, *J. Geophys. Res.*, 109, C11010, doi:10.1029/2004JC002419, 2004.
- Claustre, H., Babin, M., Merien, D. Ras., J., Prieur, L., Dallot, S., Prasil, O., Dousova, H., and Moutin, T.: Toward a taxon-specific parameterization of bio-optical models of primary production: A case study in the North Atlantic, *J. Geophys. Res.-Oceans*, 110, C07S12, doi:10.1029/2004JC002634, 2005.
- Cullen, J. J.: The deep chlorophyll maximum: comparing vertical profiles of chlorophyll a, *Canadian Journal of Fisheries and Aquatic Sciences*, 39, 791–803, 1982.
- Doron, M., Babin, M., Mangin, A., and Hembise, O.: Estimation of light penetration, and horizontal and vertical visibility in oceanic and coastal waters from surface reflectance, *J. Geophys. Res.*, in press, 2007.
- Falkowski, P. G. and Raven, J. A.: *Aquatic Photosynthesis*, Blackwell Science, Malden, 1997.
- Gardner, W. D., Mishonov, A., and Richardson, M. J.: Global POC concentrations from in-situ and satellite data, *Deep-Sea Res. Part II-Topical Studies Oceanogr.*, 53, 718–740, 2006.
- Gordon, H. R. and McCluney, W. R.: Estimation of the depth of sunlight penetration in the sea for remote sensing, *Appl. Opt.*, 14, 413–416, 1975.
- Gregg, W. W. and Carder, K. L.: A simple spectral solar irradiance model for cloudless maritime

BGD

4, 707–745, 2007

**Proxies of biomass
for primary
production**

Y. Huot et al.

Title Page

Abstract

Introduction

Conclusions

References

Tables

Figures

◀

▶

◀

▶

Back

Close

Full Screen / Esc

Printer-friendly Version

Interactive Discussion

EGU

- atmosphere, *Limnol. Oceanogr.*, 35, 1657–1675, 1990.
- IOCCG: Remote sensing of inherent optical properties: Fundamentals, tests of algorithms, and applications. Pp. 126 in V. Stuart, ed. Reports of the international ocean-colour coordinating group. IOCCG, Dartmouth, 2006.
- 5 Jeffrey, S. W. and Humphrey, G. F.: New spectrophotometric equation for determining chlorophyll a, b c1 and c2, *Biochem. Physiol. Pflanz.*, 167, 194–204, 1975.
- Kitchen, J. C. and Zaneveld, J. R.: A three layer sphere model of the optical properties of phytoplankton, *Limnol. Oceanogr.*, 37, 1680–1690, 1992.
- 10 Lee, Z. P., Carder, K. L., Marra, J., Steward, R. G., and Perry, M. J.: Estimating primary production at depth from remote sensing, *Appl. Opt.*, 35, 463–474, 1996.
- Lewis, M. R. and Smith, J. C.: A small volume, short-incubation-time method for measurement of photosynthesis as a function of incident irradiance, *Mar. Ecol. Progress Ser.*, 13, 99–102, 1983.
- Loisel, H. and Morel, A.: Light scattering and chlorophyll concentration in case 1 waters: a reexamination, *Limnol. Oceanogr.*, 43, 847–858, 1998.
- 15 Longhurst, A. R.: *Ecological Geography of the Sea*, Academic Press, San Diego, 1998.
- Lorenzen, C. J.: A method for the continuous measurement of in vivo chlorophyll concentration, *Deep-Sea Res.*, 13, 223–227, 1966.
- MacIntyre, H. L. and Cullen, J. J.: Using cultures to investigate the physiological ecology of microalgae in R. M. Anderson, ed. *Algal Culturing Techniques*. Academic Press, 2005.
- 20 MacIntyre, H. L., Kana, T. M., Anning, T., and Geider, R. J.: Photoacclimation of photosynthesis irradiance response curves and photosynthetic pigments in microalgae and cyanobacteria, *J. Phycol.*, 38, 17–38, 2002.
- Mantoura, R. F. C. and Llewellyn, C. A.: The rapid determination of algal chlorophyll and carotenoid pigments and their breakdown products in natural waters by reverse-phase high-performance liquid chromatography, *Analytica Chimica Acta*, 151, 297–314, 1983.
- 25 Maritorena, S., Siegel, D. A., and Peterson, A. R.: Optimization of a semianalytical ocean color model for global-scale applications, *Appl. Opt.*, 41, 2705–2714, 2002.
- Marra, J., Trees, C. C., and O'Reilly, J. E.: Phytoplankton pigment absorption: A strong predictor of primary productivity in the surface ocean, *Deep Sea Res. part 1*, 54, 155–163, 2007.
- 30 Morel, A.: Light and marine photosynthesis: a spectral model with geochemical and climatological implications, *Progress Oceanogr.*, 26, 263–306, 1991.
- Morel, A.: Optical modeling of the upper ocean in relation to its biogenous matter content (case

BGD

4, 707–745, 2007

**Proxies of biomass
for primary
production**

Y. Huot et al.

Title Page

Abstract

Introduction

Conclusions

References

Tables

Figures

◀

▶

◀

▶

Back

Close

Full Screen / Esc

Printer-friendly Version

Interactive Discussion

EGU

- 1 waters), *J. Geophys. Res.*, 93, 10 749–10 768, 1988.
- Morel, A.: Diffusion de la lumière par les eaux de mer. Resultats expérimentaux et approche théorique., AGARD lectures series, 3.1.1–3.1.76, 1973.
- Morel, A. and Ahn, Y.-H.: Optics of heterotrophic nanoflagellates and ciliates: A tentative assessment of their scattering role in oceanic waters compared to those of bacterial and algal cells, *J. Mar. Res.*, 49, 177–202, 1991.
- Morel, A., and Bricaud, A.: Inherent properties of algal cells including picoplankton: Theoretical and experimental results. Pp. 521–559, in: *Photosynthetic Picoplankton*, edited by: Platt, T. and Li, W. K. W., 1986.
- Morel, A., Gentili, B., Claustre, H. Babin., M., Bricaud, A., Ras, J., and Tieche, F.: Optical properties of the “clearest” natural waters, *Limnol. Oceanogr.*, 52, 217–229, 2007.
- Morel, A., and Maritorea, S.: Bio-optical properties of oceanic waters: A reappraisal, *J. Geophys. Res.*, 106, 7163–7180, 2001.
- O’Reilly, J. E., Maritorea, S., Mitchell, B. G., Siegel, D. A., Carder, K. L., Garver, S. A., Kahru, M., and McClain, C. R.: Ocean color chlorophyll algorithm for SeaWiFS, *J. Geophys. Res.*, 103, 24 937–24 953, 1998.
- Oubelkheir, K., Claustre, H., Sciandra, A., and Babin, M.: Bio-optical and biogeochemical properties of different trophic regimes in oceanic waters, *Limnol. Oceanogr.*, 50, 1795–1809, 2005.
- Perry, M. J.: Measurements of phytoplankton absorption other than per unit of chlorophyll a. Pp. 107-116 in: *Ocean Optics*, edited by: Spinrad, R. W., Carder, K. L., and Perry, M. J., Oxford University Press, New York, 1994.
- Platt, T., Gallegos, C. L., and Harrison, W. G.: Photoinhibition of photosynthesis in natural assemblages of marine phytoplankton, *J. Mar. Res.*, 38, 687–701, 1980.
- Platt, T. and Sathyendranath, S.: Spatial structure of pelagic ecosystem processes in the global ocean, *Ecosystems*, 2, 384–394, 1999.
- Roesler, C. S.: Spectral beam attenuation coefficient retrieved from ocean color inversion, *Geophys. Res. Lett.*, 30, 1468, doi:1410.1029/2002GL016185, 2003.
- Siegel, D. A., Dickey, T. D., Washburn, L., Hamilton, M. K., and Mitchell, B. G.: Optical determination of particulate abundance and production variations in the oligotrophic ocean, *Deep Sea Res.*, 36, 211–222, 1989.
- Smith, H. J.: Earth Science: getting a fix on fixation, *Science*, 307, doi:10.1126/science.1307.5710.1647a, 2005.

BGD

4, 707–745, 2007

**Proxies of biomass
for primary
production**

Y. Huot et al.

Title Page

Abstract

Introduction

Conclusions

References

Tables

Figures

◀

▶

◀

▶

Back

Close

Full Screen / Esc

Printer-friendly Version

Interactive Discussion

EGU

- Sokal, R. R. and Rohlf, F. J.: Biometry the principles and practice of statistics in biological research, W.H. Freeman and Company, New York, 1995.
- Stramski, D., Boss, E., Bogucki, D., and Voss, K. J.: The role of seawater constituents in light backscattering in the ocean, *Progress Oceanogr.*, 61, 27–56, 2004.
- 5 Stramski, D., Reynolds, C. S., Kahru, M., and Mitchell, B. G.: Estimation of particulate organic carbon in the ocean from remote sensing, *Science*, 285, 239–242, 1999.
- Sukenic, A., Bennett, J., and Falkowski, P. G.: Light-saturated photosynthesis – limitation by electron transport or carbon fixation, *Biochimica et Biophysica Acta*, 891, 205–215, 1987.
- 10 Sullivan, J. M., Twardowski, M. S. Zaneveld, J. R., Moore, C., Barnard, A., Donaghay, P. L., and Rhoades, B.: The hyperspectral temperature and salinity dependencies of absorption by water and heavy water in the 400–750 nm spectral range, *Appl. Opt.*, 45, 5294–5309, 2006.
- Twardowski, M. S., Sullivan, J. M., Donaghay, P. L., and Zaneveld, J. R.: Microscale quantification of the absorption by dissolved and particulate material in coastal waters with an ac-9, *J. Atmos. Oceanic Technol.*, 16, 691–707, 1999.
- 15 Yentsch, C. S. and Menzel, D. W.: A method for the determination of phytoplankton chlorophyll and phaeophytin by fluorescence, *Deep-Sea Res.*, 10, 221–231, 1963.
- Zaneveld, J. R. V., Kitchen, J. C., and Moore, C. C.L: The scattering error correction of reflecting tube absorption meters. Pp. 44–55, edited by: Ackelson, S., *Ocean Optics XII. Proc. SPIE* 2258. 1994.

BGD

4, 707–745, 2007

**Proxies of biomass
for primary
production**

Y. Huot et al.

Title Page

Abstract

Introduction

Conclusions

References

Tables

Figures

◀

▶

◀

▶

Back

Close

Full Screen / Esc

Printer-friendly Version

Interactive Discussion

EGU

Table 1. Summary of a) sources of variability in the photosynthetic parameters that are not accounted for by the normalization to different biomass proxies (always listed as point #1 below), and b) principal origin of this variability (presented below as point #2). See Falkowski and Raven (1997) for details regarding the absorption based proxies; further explanation of the scattering based proxies are developed in the text.

Absorption-related biomass proxies			
Tchl _a	\bar{a}_{ps}	\bar{a}_{phy}	Fluorescence
<p>P_{max}</p> <p>1) ratio : $n_{slowest}/Tchl_a$.</p> <p>2) Photoacclimation and nutritional status. Expected to decrease with increasing growth irradiance and nutrient availability. Also influenced by species composition.</p>	<p>1) ratio : $n_{slowest}/\bar{a}_{ps}$.</p> <p>2) The same sources as Tchl_a, plus packaging effects and pigment composition.</p>	<p>1) ratio : $n_{slowest}/\bar{a}_{phy}$.</p> <p>2) The same sources as \bar{a}_{ps}.</p>	<p>1) ratio : $n_{slowest}/(\bar{a}_{ps}\Phi_f^{ps})$ where Φ_f^{ps} is the quantum yield of fluorescence.</p> <p>2) Same sources as for \bar{a}_{ps} plus variability due to the quantum yield of fluorescence.</p>
<p>α</p> <p>1) Chlorophyll specific absorption coefficient ($\bar{a}_{ps}^* = \bar{a}_{ps}/Tchl_a$).</p> <p>2) Pigment composition and packaging, and thus the physiological status and species composition.</p>	<p>1) Physiologically none.</p> <p>2) Methodologically, it may be susceptible to larger variability than expected due to significant errors in the estimation of \bar{a}_{ps}.</p>	<p>1) ratio: $\bar{a}_{ps}/\bar{a}_{phy}$</p> <p>2) Photoacclimation, nutritional status and species composition. Also affected by errors in the determination of phytoplankton absorption.</p>	<p>1 ratio: $\bar{a}_{ps}/\bar{a}_{ps}\Phi_f^{ps}$</p> <p>2) Additional variability in Φ_f^{ps} and different the measuring irradiance used to «weight» \bar{a}_{ps}, and, hence, on the pigment composition.</p>
Scattering-related biomass proxies			
b_p (or c_p)		b_{bp}	biovolumes
<p>P_{max}</p> <p>1) $\left(\frac{n_{slowest}}{b_{phy}} \right) \left(\frac{b_{phy}}{b_{phy} + b_{bact} + b_{het} + b_{vir} + b_{min} + b_{bub} + b_{org}} \right)$</p> <p>2) See text for further details.</p>		<p>1) Same equation as for b_p (replacing b_p by b_{bp}).</p> <p>2) See text for further details.</p>	<p>1) The intracellular $n_{slowest}$ concentration.</p> <p>2) Physiological status and species composition. Methodologically limited by the accuracy in volume determination and cellular volumes observed by flow cytometry.</p>
<p>α</p> <p>1) $\left(\frac{\bar{a}_{ps}}{b_{phy}} \right) \left(\frac{b_{phy}}{b_{phy} + b_{bact} + b_{het} + b_{vir} + b_{min} + b_{bub} + b_{org}} \right)$</p> <p>2) See text for further details.</p>		<p>1) Same equation as for b_p (replacing b_p by b_{bp}).</p> <p>2) See text for further details.</p>	<p>The volume specific absorption coefficient.</p> <p>Dependent on physiological status. Same methodological problems as above.</p>

Title Page

Abstract Introduction

Conclusions References

Tables Figures

◀ ▶

◀ ▶

Back Close

Full Screen / Esc

Printer-friendly Version

Interactive Discussion

Table 2. Stepwise fit results for P_{\max} vs different indices of biomass. Values represent the fitted coefficients for each variable. NU is used for “Not Used in the fit”.

	Tchla	a_{ps}	a_{phy}	fluo	$b(650)$	$b_b(650)$
Intercept	0.231	2.37	2.67	0.668	3.21	12.20
Log ₁₀ (Biomass)	1.20	−4.23E-03	−5.23E-3	−9.72E-3	2.98	5.15
Log ₁₀ (Biomass) ²	8.46E-2	7.94E-06	1.16E-5	2.63E-5	0.659	0.597
Depth	−6.45E-3	3.25E-02	3.30E-2	NU	NU	NU
Depth ²	1.24E-5	NU	NU	NU	5.80E-6	1.00E-5
T	1.75E-2	NU	NU	NU	−1.52E-1	−2.80E-1
T ²	NU	3.63E-02	NU	NU	4.07E-3	7.33E-3
Log ₁₀ (E_{growth}) [†]	NU	NU	NU	NU	NU	NU
Log ₁₀ (PAR _{theo}) [§]	NU	NU	NU	NU	NU	3.63E-2
Log ₁₀ (PAR _{theo}) ²	NU	1.77	1.92	1.11	NU	NU
Log ₁₀ (NO ₃)	NU	0.140	0.163	NU	−7.12E-2	NU
RMSE	0.13	0.15	0.16	0.18	0.21	0.23
MAPE	0.25	0.28	0.30	0.35	0.42	0.46
R ²	0.93	0.91	0.90	0.88	0.83	0.80

† E_{growth} is the mean PAR irradiance during daylight ($\mu\text{mol photon m}^{-2} \text{s}^{-1}$) at the sampling depth over the three days previous to the sampling day. It is calculated using the incident irradiance measured on the ship and the attenuation coefficient measured at the station.

§ PAR_{theo} is the mean PAR irradiance calculated using the Gregg and Carder (1990) model at the sampling depth for the sampling day, and therefore does not account for cloudiness.

**Proxies of biomass
for primary
production**

Y. Huot et al.

Title Page

Abstract

Introduction

Conclusions

References

Tables

Figures

◀

▶

◀

▶

Back

Close

Full Screen / Esc

Printer-friendly Version

Interactive Discussion

**Proxies of biomass
for primary
production**

Y. Huot et al.

Title Page

Abstract

Introduction

Conclusions

References

Tables

Figures

◀

▶

◀

▶

Back

Close

Full Screen / Esc

Printer-friendly Version

Interactive Discussion

Table 3. Stepwise fit results for α vs different indices of biomass. Values represent the fitted coefficients for each variable. NU is used for “Not Used in the fit”.

	Tchl _a	$b(650)$	$b_b(650)$	a_{ps}	a_{phy}	fluo
Intercept	−1.38	0.903	21.5	1.32	1.40	−1.20
Log ₁₀ (Biomass)	1.36	3.90	9.34	1.93	1.29	1.47
Log ₁₀ (Biomass) ²	NU	0.890	1.19	0.117	NU	NU
Depth	NU	NU	NU	NU	−1.11E-2	−3.43E-3
Depth ²	5.18E-6	2.15E-5	2.84E-5	1.288E-5	4.75E-5	2.75E-5
T	NU	NU	−0.651	NU	1.21E-1	−1.14E-2
T ²	NU	2.86E-4	1.55E-2	4.49E-4	NU	NU
Log ₁₀ (E _{growth}) †	−3.18E-2	NU	NU	NU	2.51E-4	NU
Log ₁₀ (PAR _{theo}) [§]	NU	NU	0.149	NU	NU	NU
Log ₁₀ (PAR _{theo}) ²	NU	−2.10E-2	−3.04E-2	NU	NU	NU
Log ₁₀ (NO ₃)	NU	NU	3.37E-2	NU	−1.167E-2	1.45E-2
RMSE	0.20	0.31	0.32	0.22	0.23	0.21
MAPE	0.40	0.68	0.69	0.44	0.46	0.41
R ²	0.90	0.78	0.76	0.89	0.88	0.90

†See Table 2.

§ See Table 2.

Proxies of biomass for primary production

Y. Huot et al.

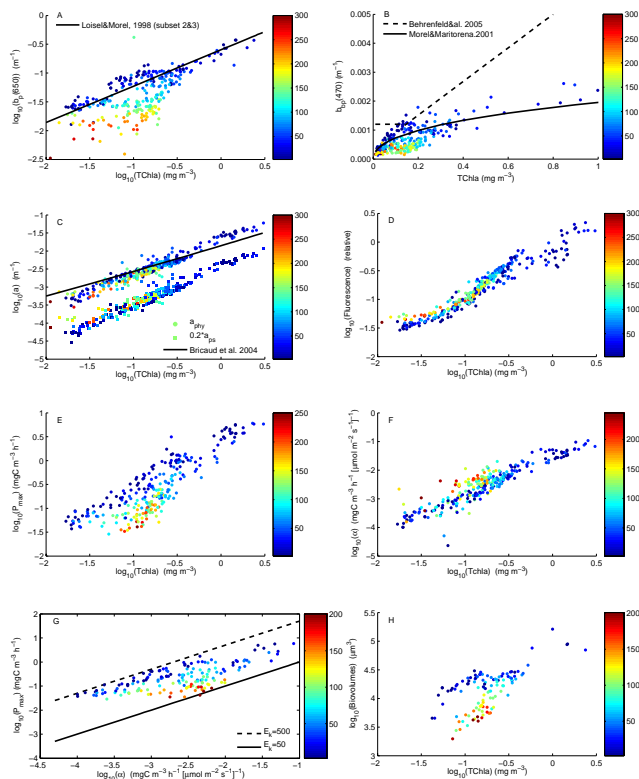


Fig. 1. Comparison of different estimators of phytoplankton biomass obtained during the BIOSOPE cruise with available statistics for case 1 waters. **(A)** Particulate scattering coefficient at 650 nm vs Tchl_a (sum of chlorophyll a and divinyl chlorophyll a, **(B)** Backscattering coefficient at 470 nm vs Tchl_a, **(C)** Phytoplankton and photosynthetic absorption multiplied by 0.2 (allows it to be discerned from the former) weighted by the photosynthetron irradiance spectra vs Tchl_a, **(D)** In situ fluorescence vs Tchl_a, **(E)** P_{\max} vs Tchl_a, **(F)** α vs Tchl_a, **(G)** P_{\max} vs α , lines are for two extreme saturation irradiances (E_k) for photosynthesis, **(H)** Biovolume obtained from a calibrated flow cytometer vs Tchl_a. Colorscale represents depth.

Title Page

Abstract

Introduction

Conclusions

References

Tables

Figures

◀

▶

◀

▶

Back

Close

Full Screen / Esc

Printer-friendly Version

Interactive Discussion

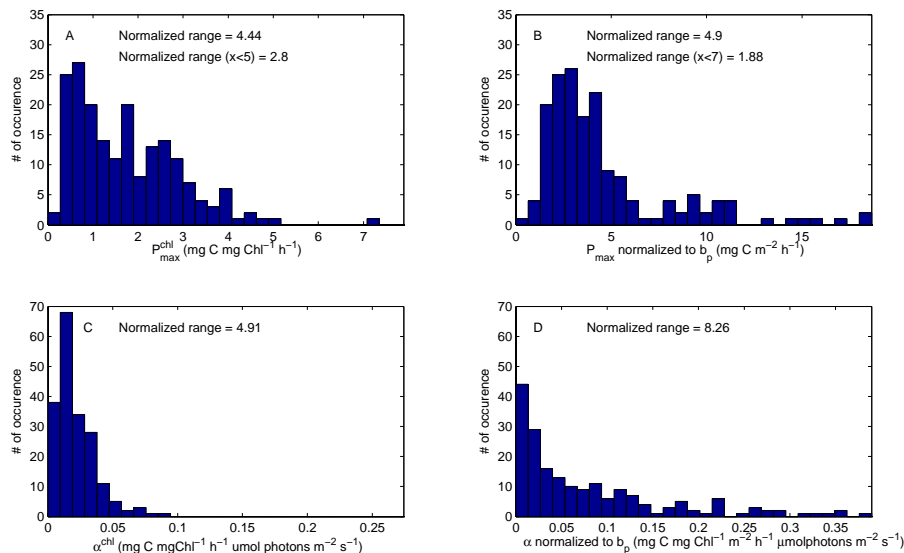


Fig. 2. Histograms of the photosynthetic parameters measured during the BIOSOPE cruise. **(A)** P_{\max}^{chl} , **(B)** P_{\max} normalized to b_p , **(C)** α^{chl} , **(D)** α normalized to b_p . The normalized range was calculated as $(\min(x) - \max(x)) / \text{median}(x)$, where x is the normalized photosynthetic parameter. It provides a rough guide to compare the variability between the different panels. For panel A and B, two ranges are given, one for the whole dataset, as in the other panels, and one for normalized P_{\max} smaller than $5 \text{ mg C mg Chl}^{-1} \text{ h}^{-1}$ for A (excluding one high point) and $7 \text{ mg C m}^{-2} \text{ h}^{-1}$ for B (focusing on the “normal” region of the distribution). The abscissa are scaled such that the ratio of the maximum of the axis to the minimum value of the data are equal (for each row independently).

[Title Page](#)
[Abstract](#)
[Introduction](#)
[Conclusions](#)
[References](#)
[Tables](#)
[Figures](#)
[⏪](#)
[⏩](#)
[◀](#)
[▶](#)
[Back](#)
[Close](#)
[Full Screen / Esc](#)
[Printer-friendly Version](#)
[Interactive Discussion](#)

Proxies of biomass for primary production

Y. Huot et al.

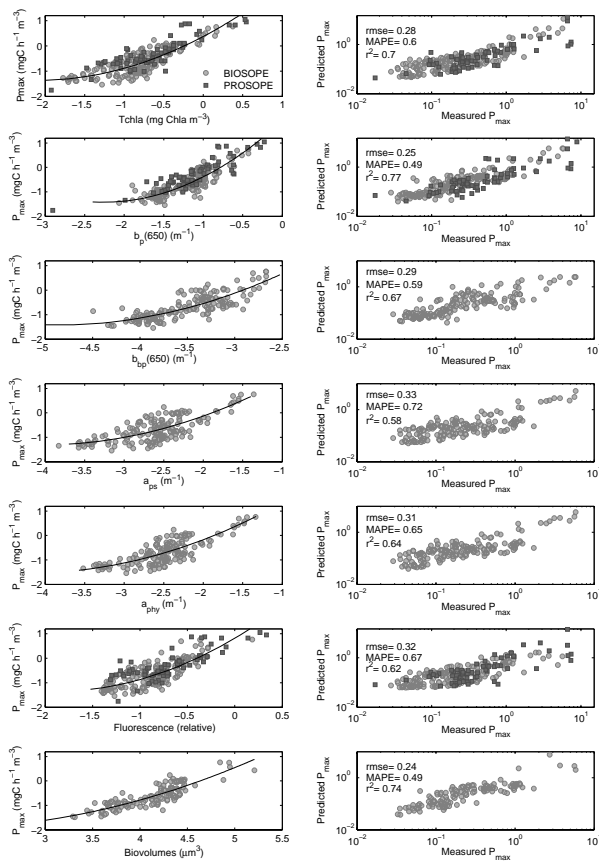


Fig. 3. Relationships between seven estimators of photosynthetic biomass and P_{max} . Left Column: P_{max} vs the different estimators. The black line represents the best fit second order polynomial. Right column: Measured and estimated P_{max} using the best fit line in the left column. Also shown are the statistics of the predictions.

Title Page

Abstract

Introduction

Conclusions

References

Tables

Figures

◀

▶

◀

▶

Back

Close

Full Screen / Esc

Printer-friendly Version

Interactive Discussion

Proxies of biomass for primary production

Y. Huot et al.

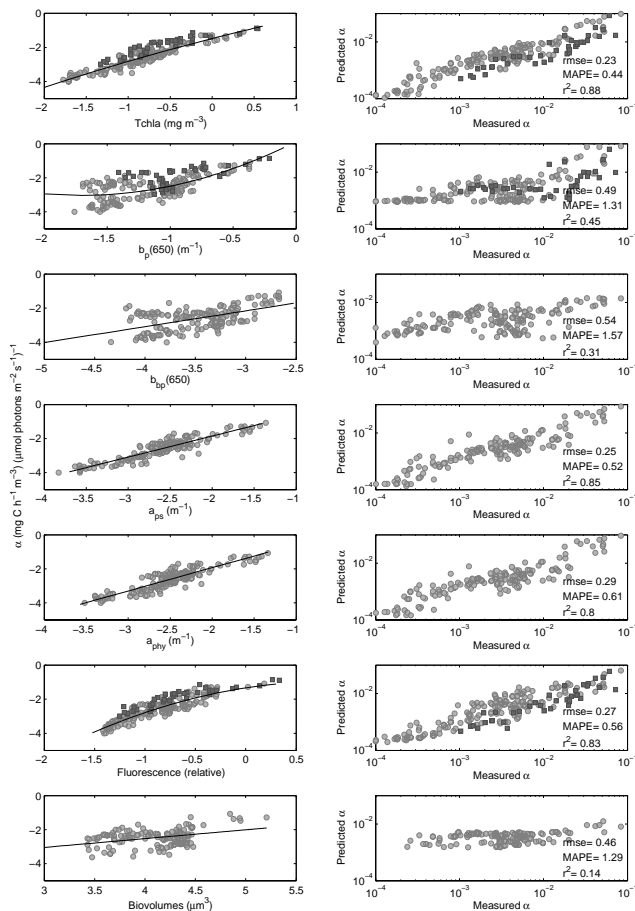


Fig. 4. Relationships between seven estimators of photosynthetic biomass and α . Left Column: α versus the different estimators. The black line represents the best fit second order polynomial. Right column: Measured and estimated α using the best fit line in the left column. Also shown are the statistics of the predictions.

Title Page

Abstract

Introduction

Conclusions

References

Tables

Figures

◀

▶

◀

▶

Back

Close

Full Screen / Esc

Printer-friendly Version

Interactive Discussion

Proxies of biomass
for primary
production

Y. Huot et al.

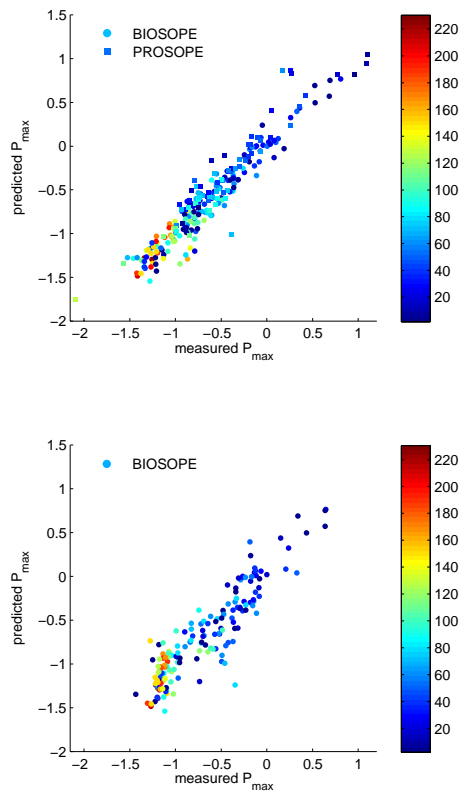


Fig. 5. Prediction of P_{\max} using several variables. **(A)** Using $Tchl_a$ as the biomass index and other variables as given in Table 2. **(B)** Same as *a* except using b_p as the biomass proxy.

Title Page

Abstract

Introduction

Conclusions

References

Tables

Figures

◀

▶

◀

▶

Back

Close

Full Screen / Esc

Printer-friendly Version

Interactive Discussion

Proxies of biomass
for primary
production

Y. Huot et al.

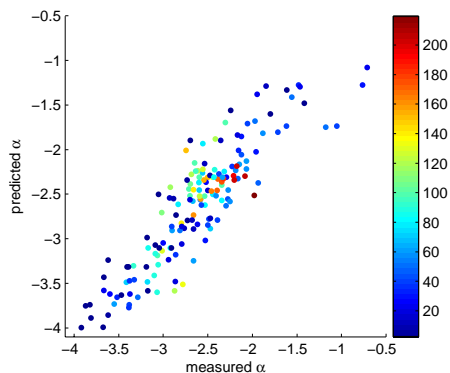
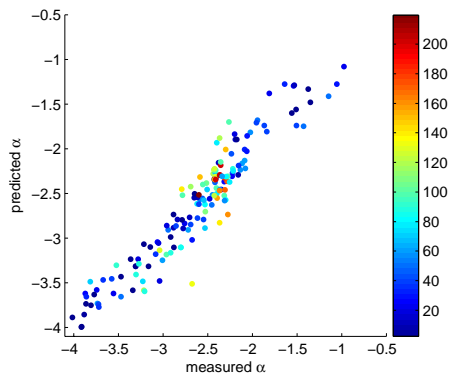


Fig. 6. Prediction of α using several variables. **(A)** Using Tchla as the biomass index and other variables as given in Table 3. **(B)** Same as (A) except using b_p as the biomass proxy.

Title Page

Abstract

Introduction

Conclusions

References

Tables

Figures

◀

▶

◀

▶

Back

Close

Full Screen / Esc

Printer-friendly Version

Interactive Discussion